Supplementary information: Stimulated Raman Scattering Imaging of Atomically Thin Layers and a Strained Nanotent of Hexagonal Boron Nitride

Kazuhiro Kuruma[1], Momoko Onodera[2], Shun Takahashi[3], Ichiro Takahashi[4], Yijin Zhang[2], Tomoki Machida[2], and Yasuyuki Ozeki[1,3]

[1]Research Center for Advanced Science and Technology, The University of Tokyo, Meguro-ku, Tokyo 153-8505, Japan
[2]Institute of Industrial Science, The University of Tokyo, Meguro-ku, Tokyo 153-8505, Japan
[3]Department of Electrical Engineering and Information Systems, The University of Tokyo, Bunkyo-ku, Tokyo 113-8656, Japan
[4]Department of Electrical and Electronic Engineering, The University of Tokyo, Bunkyo-ku, Tokyo 113-8656, Japan

1. Vibrational imaging of 1–4 layer h-BN

Figures S1(a) and (b) show enlarged SRS images of the same 1–4L h-BN, as that shown in Fig. 2(b) in the main text, measured at two different wavenumbers of 1363 cm^{-1} (vibrational on-resonance of the E_{2g} mode) and 1389 cm^{-1} (vibrational off-resonance), respectively. The conditions of the SRS measurement are the same as that shown in Fig. 2(b) in the main text. The 1–4L h-BN can be observed under the on-resonance condition while they are not visible under the off-resonance, indicating that our SRS system demonstrates the vibrational imaging of 1–4L h-BN.

In addition to the visualization of the layer number dependence of SRS intensities, the wrinkles induced by our transfer process can be clearly observed in the 1-4L h-BN. Figure S1(c) shows the SRS intensity profile across the visible wrinkles (corresponding to the solid line shown in Fig. S1(a)), exhibiting a clear intensity contrast between the wrinkles and the flat area. This result also suggests that our SRS approach could be useful for investigating wrinkles formed in thin 2D materials. The enhanced Raman signals on the wrinkles could be attributed to factors including multilayer stacking or optical interference within the multilayer structures of h-BN/air/substrate[1]. However, further detailed studies are necessary to clarify the underlying mechanism.

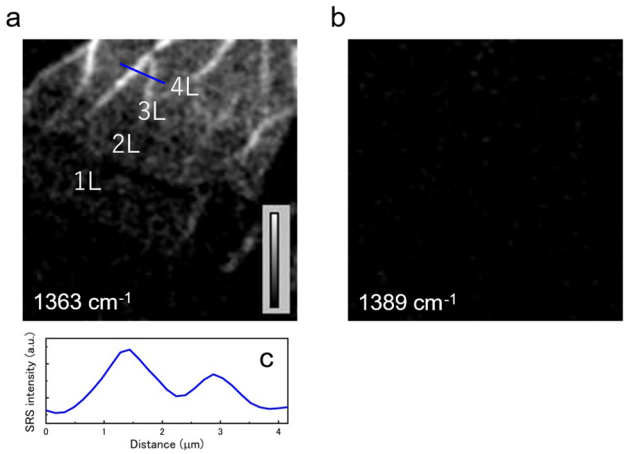

Fig. S1 SRS images of the 1–4 layer (L) h-BN measured at (a) 1363 cm^{-1} and (b) 1389 cm^{-1}. The images are denoised by a 2 × 2 pixels averaging kernel method and a Gaussian blur filter with a sigma value of 1.0. (c) Cross section of the wrinkles corresponding to the solid line shown in (a).

2. Measured linewidths of SRS spectra for 1–4 layer h-BN

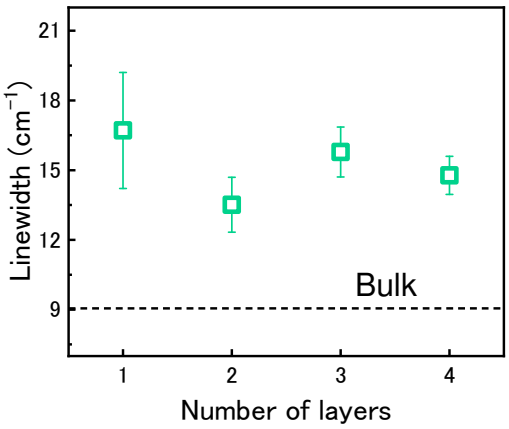

Fig. S2 Linewidth (full width at half maximum) extracted from the SRS spectra shown in Fig. 2(d) in the main text, as a function of the number of layers. The error bars represent the standard deviation of the curve fitting with a Lorentzian function.

3. Calculation of radial and circumferential strain components

The radial and circumferential strain components (ε_r and ε_θ) as a function of the radial position (r) for the tent are given by the following equations [2]:

$$\varepsilon_r = \begin{cases} A(\nu)\dfrac{{h_0}^2}{a^2}\left[1-\dfrac{1+\nu-2\alpha\nu}{2\alpha-1-\nu}\left(\dfrac{r}{a}\right)^{2\alpha-2}\right]+\dfrac{u_s}{a}, & r\le a \\ -\dfrac{au_s}{r^2}, & r>a \end{cases}, \tag{S1}$$

$$\varepsilon_\theta = \begin{cases} A(\nu)\dfrac{{h_0}^2}{a^2}\left[1-\left(\dfrac{r}{a}\right)^{2\alpha-2}\right]+\dfrac{u_s}{a}, & r\le a \\ \dfrac{au_s}{r^2}, & r>a \end{cases}. \tag{S2}$$

where, $A(\nu) = \{[\alpha(2\alpha-1-\nu)]/[8(\alpha-1)]\}$. h_0 and a are the central height and radius of the tent, respectively. u_s is a constant relevant to the slippage at the edge of the tent, which leads to two boundary conditions of 2D materials-substrate interface: Strong shear limit (2D materials are fully clamped on substrate) and weak-shear limit (2D materials slide on substrate). u_s for each limit is given by [2]:

$$u_s = \begin{cases} 0, & \text{strong-shear limit} \\ -\dfrac{\alpha(1+\nu)}{8}\dfrac{{h_0}^2}{a}, & \text{weak-shear limit} \end{cases}. \tag{S3}$$

In our calculation of the strains, we assume the weak-shear limit, since the h-BN flake with the tent is placed on the surface coating with a low friction on a cover glass. As can be seen in Fig. S3, the theoretical fitting using the weak-shear limit (red curve) shows better fitting to the measured peak shifts compared to that using the strong-shear limit (blue curve). Using Eqs. (S1–S3) and Eq. (1) in the main text, we fitted the experimental data with the theoretical model in Fig. 3(i) in the main text.

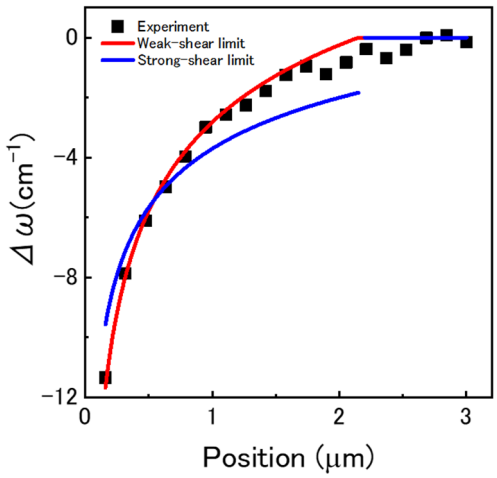

Fig. S3 Measured peak shifts $\Delta\omega$ near the strained tent as a function of radial position r.

References

[1] K.Y. Lee, T. Lee, Y.G. Yoon, Y.J. Lee, C.H. Cho, H. Rho, Appl Surf Sci 604 (2022) 154489.

[2] Z. Dai, Y. Hou, D.A. Sanchez, G. Wang, C.J. Brennan, Z. Zhang, L. Liu, N. Lu, Phys Rev Lett 121 (2018) 266101.